Dual Fluorescence and Multiple Charge Transfer Nature in Derivatives of *N*-Pyrrolobenzonitrile

Claudia Cornelissen-Gude and Wolfgang Rettig*

W. Nernst Institut für Physikalische und Theoretische Chemie, Humboldt-Universität zu Berlin, Bunsenstr. 1, D-10117 Berlin, Germany

Received: February 26, 1998; In Final Form: May 27, 1998

N-Pyrrolobenzonitrile (PBN), its ester derviative PBAEE, and a more twisted model compound DPBN have been compared regarding absorption and fluorescence properties. A long wavelength absorption shoulder in DPBN has been assigned to the charge transfer (CT) state. In polar solvents, single-fluorescence bands with a strong solvatochromic effect establish a CT nature of the emission for all compounds. The long radiative lifetime (ca. 130 ns for PBN, 700 ns for DPBN in CH_2Cl_2) points to a forbidden emission, and the 5-fold longer value for DPBN indicates a difference in CT nature tentatively assigned to conformations differing in the twist angle. Even in low-temperature polar solvent glasses, the single-fluorescence band of PBN is of CT nature and develops into a dual fluorescence by thermal activation. Also in alkanes, the increased fluorescence rate constants and the temperature effect on spectral structuring indicate emission from an equilibrium involving a CT state with an unstructured spectrum and a less polar locally excited state with structured emission.

1. Introduction

Spectroscopic studies of donor/acceptor substituted benzenes often reveal the phenomenon of dual fluorescence or exhibit emission bands with anomalously large Stokes shifts. In general, large Stokes shifts can be produced by molecules possessing excited-state relaxation processes where large amplitude motions are involved. TICT (twisted intramolecular charge transfer) compounds represent a particular class of molecules exhibiting dual emission or anomalous Stokes shifts.[1−4] According to the TICT model, the fluorescence originates from the primarily excited "locally excited" (LE) state as well as from a charge transfer (CT) state accessible only by an adiabatic photoreaction from LE, which includes a rotational motion around the bond linking the donor and acceptor moieties. If there is no energy barrier separating the precursor and product species, the excited-state relaxation can occur extremely rapidly. In this case, only long wavelength emission from the CT product state may be observable. This TICT emission process is usually connected with a reduced value of the transition moment due to the small π-overlap of the strongly twisted arrangement of chromophores.[1,4,5] Dimethylaminobenzonitrile (DMABN, Scheme 1) represents the prototype TICT compound exhibiting the phenomenon of dual fluorescence.[1,6] Furthermore, a number of derivatives show comparable spectroscopic features.[3,4,7] In this paper we want to draw the parallels to the closely related pyrrolobenzonitriles, which instead of a saturated dimethylamino group possess the even better donor moiety pyrrol. We want to present a detailed investigation of the fluorescence spectra and corresponding photophysical data at various temperatures of the pyrrolobenzonitriles depicted in Scheme 1b−d.

The chemical structure of the compounds investigated (b−d) resembles on one hand the TICT system DMABN (a), and on the other hand their donor/acceptor capabilities are comparable with those of $PBMes_2$ (e), a compound which shows an enormous Stokes shift even in nonpolar solvents.[8,9] $PBMes_2$ differs from the investigated pyrrolobenzonitriles by the strength of the acceptor unit, which is diminished for the latter compounds.[10]

SCHEME 1

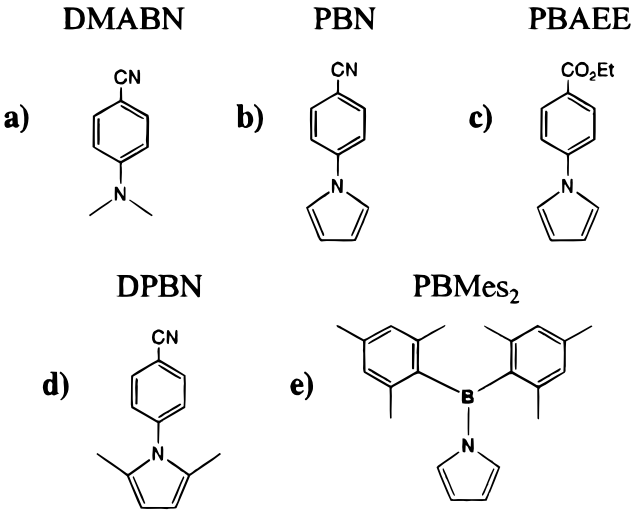

The investigation of the spectroscopic behavior of PBN, PBAEE, and DPBN includes a variation of the polarity as well as temperature-dependent effects. Previous studies at room temperature for some of the pyrrolobenzonitriles revealed the connection with donor/acceptor strength and the twist angle.[7,11,12] On the other hand, due to the particular electronic properties of pyrrol with a node through N in the highest molecular orbital (HOMO), special features can be expected and large charge separation is even possible for planar geometries.[13]

2. Experimental Section

The compounds were synthesized using the procedures described in refs 11 and 12. The absence of possible traces of

S1089-5639(98)01306-1 CCC: $15.00
Published on Web 09/12/1998

impurities was confirmed by high-performance thin layer chromatography (HPTLC).[14] Absorption spectra were measured on a Cary 17 spectrometer, and quantum-corrected fluorescence spectra (concentrations $< 10^{-4}$ M) were measured on a Perkin-Elmer 650-60 fluorimeter.

Basic Blue 3 [15] was used as quantum counter to extend the correction range of the emission up to 700 nm. Fluorescence quantum yields were determined relative to a solution of quinine bisulfate in 0.1 N H_2SO_4 ($\phi_f = 0.515$)[16] and corrected for the refractive index of the solvents. Fluorescence spectra, measured in aerated solutions, were independent of concentration (o.d. $\approx$ 0.05−0.8) and excitation wavelength. The determination of low-temperature fluorescence quantum yields took into account the temperature dependence of the refractive index as well as the increasing solvent contraction (density increase) with decreasing temperature.

Fluorescence decay times of the aerated solutions were determined with the time-correlated single-photon counting (SPC) technique[17] using equipment described in detail elsewhere.[18] Comparative measurements with polarization filters set to the magic angle position were carried out but were not used as standard condition because of the low intensity of the emission. Synchrotron radiation from the Berlin electron storage ring BESSY operating in the single bunch mode was used for excitation.[18] The decay times were fitted using the iterative reconvolution procedure (Marquard algorithm), which allowed a time resolution down to 0.1 ns and a relative precision of about 0.1 ns.

Solvents for fluorescence spectroscopy were of Merck Uvasol quality, with the exception of butyronitrile, and were used without further purification. Butyronitrile was purified by column chromatography (Al_2O_3) and repeated vacuum distillation.

3. Results

3.1. Room-Temperature Data. The absorption and emission spectra of PBN and PBAEE are almost identical in the amount of Stokes shift, whereas the fluorescence data of the sterically hindered dimethyl-substituted compound DPBN differ substantially with strongly red-shifted spectra even in nonpolar and weakly polar solvents (Figures 1 and 2).

The fluorescence of all three compounds shows significant solvatochromic effects, indicating a high charge transfer character of the emitting state. The absorption bands, however, do not shift significantly in solvents of increasing polarity. Despite the fact that the methyl substituents in ortho position of the pyrrole moiety enhance the donor capability,[9,11,12] the main absorption maximum of DPBN is clearly blue-shifted in comparison to the band maxima of PBN and PBAEE.

The molecular absorption coefficients were determined for PBAEE and DPBN in *n*-hexane as $\epsilon(\lambda_{286}^{max}) = 22\,000\ M^{-1}cm^{-1}$ and $\epsilon(\lambda_{275}^{max}) = 10\,000\ M^{-1}cm^{-1}$ respectively, which differs by a factor of about 2. The blue shift and the reduction of absorption intensity are typical for twisted compounds. Using Webster's approach[19] we can derive the ground-state twist angle $\langle\varphi\rangle$ by using eq 1.

$$\epsilon/\epsilon_{Ref} = \cos^2\langle\varphi\rangle \tag{1}$$

With PBAEE as the reference compound, $\langle\varphi\rangle$ is found to be 48° for DPBN. This value corresponds well to the twist angles of 50° determined by photoelectron spectroscopy.[12] In contrast to PBN, a weak shoulder in the red edge of the absorption

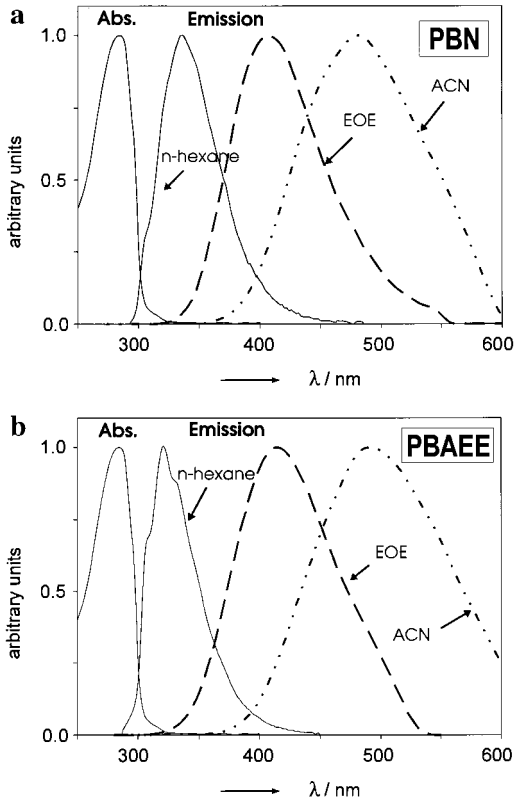

Figure 1. Absorption and fluorescence spectra of (a) PBN and (b) PBAEE at room temperature in solvents of different polarity.

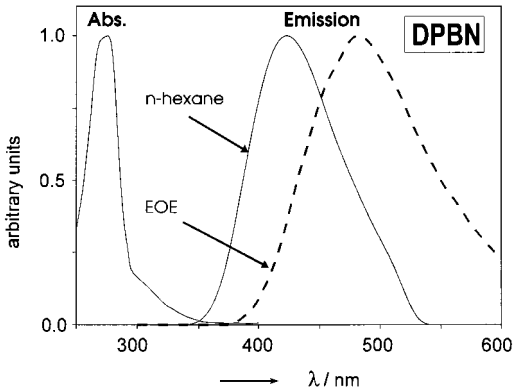

Figure 2. Absorption and fluorescence spectra of DPBN at room temperature in solvents of different polarity.

spectra can be observed for DPBN, which can be interpreted as a hint for a hidden transition.

The fluorescence decay curves are monoexponential, which allows the evaluation of radiative and nonradiative rate constants according to eqs 2 and 3. In eq 2, k_{nr}^{tot} corresponds to the sum

$$k_f = \phi_f/\tau_f \tag{2}$$

$$k_{nr}^{tot} = k_f(\phi_f^{-1} - 1) \tag{3}$$

of all nonradiative processes including triplet formation. The measured data and calculated photophysical rates are collected in Table 1a−c.

The comparison of spectra and rate constants of PBN and PBAEE exhibits rather similar features except in nonpolar solvents such as *n*-hexane and in protic media like water and alcohols. Whereas the emission spectrum of PBAEE in *n*-hexane shows clearly some vibronic structure, that of PBN

TABLE 1: Spectral and Photophysical Data at Room Temperature for (a) PBN, (b) PBAEE, and (c) DPBN in Solvents of Different Polarity

solvent	λ_{max}^{em}/nm	$\Delta\nu_{St}$/cm^{-1}	φ_f	τ_f/ns	k_f/s^{-1}	k_{nr}/s^{-1}
			(a) PBN[a]			
n-hexane	348	6200	0.028	2.42	1.16×10^7	4.0×10^8
diethyl ether	404	10 200	0.022	3.80	0.57×10^7	2.6×10^8
dichloromethane	426	11 500	0.022	3.10	0.72×10^7	3.2×10^8
acetonitrile	482	14 200	0.036	8.20	0.43×10^7	1.2×10^8
			(b) PBAEE[a]			
n-hexane	332	4800	0.033	1.36	2.41×10^7	7.1×10^8
diethyl ether	414	10 800	0.032	5.60	0.57×10^7	1.7×10^8
dichloromethane	434	11 900	0.036	4.50	0.79×10^7	2.1×10^8
acetonitrile	490	14 600	0.029	5.90	0.49×10^7	1.6×10^8
			(c) DPBN[b]			
n-hexane	420	12 600	0.006	2.9	1.9×10^6	3.4×10^8
dibutyl ether	450	14 100	0.010	7.1	1.5×10^6	1.4×10^8
diethyl ether	480	15 500	0.018	12.9	1.4×10^6	0.8×10^8
dichloromethane	530	17 500	0.014	10.7	1.3×10^6	0.9×10^8
acetonitrile	no fluorescence observable at 298 K ($\varphi_f < 0.001$)					

[a] $\lambda_{max}^{exc} = 286$ nm. [b] $\lambda_{max}^{exc} = 275$ nm.

TABLE 2: Spectral and Photophysical Data of PBN and PBAEE in Alcohols at 298 K

solvent	compd	λ_{max}^{exc}/nm	φ_f	τ_f/ns	$k_{nr}/10^8$ s^{-1}
HexOH	PBN	449	0.043	7.1	1.3
	PBAEE	486	0.011	1.5	6.6
PropOH	PBN	468	0.029	5.6	1.6
	PBAEE	494	0.004	0.7	14.2
EtOH	PBN	478	0.022	4.3	2.3
	PBAEE	496	0.002	*a*	34.1[b]
MeOH	PBN	493	0.008	2.0	4.9
	PBAEE	520	<0.001	*a*	85.4[b]

[a] Not observable. [b] Calculated using $k_f = 6.4 \times 10^6$ determined in PropOH and HexOH.

remains much less structured (Figure 1a,b). A further difference concerns the magnitude of the fluorescence rate constant in *n*-hexane, which is twice as large for the ester PBAEE than for the nitrile PBN, (Table 1) whereas in the other solvents, the values are nearly identical.

In contrast to the general spectroscopic observation in aprotic solvents, a strong fluorescence quenching has been detected for PBAEE in protic solvents, which is much less pronounced for PBN (Table 2). The fluorescence quenching increases with decreasing chain length—i.e., increasing acidity and polarity—of the alcohol. Possibly, there are specific interactions present, of the type solvent−ester group, leading to the significant enhancement of the nonradiative properties of PBAEE in protic solutions.

As mentioned before, the fluorescence behavior of the dimethyl-substituted compound DPBN differs remarkably from that of PBN and PBAEE. The spectra of DPBN exhibit larger Stokes shifts, about 13 000 cm^{-1} (measured from the absorption maximum) even in nonpolar solvents such as *n*-hexane (Figure 2, Table 1c).

The larger fluorescence red shifts can be explained by a lower energy of the charge transfer state due to the enhanced donor capability of the dimethyl-substituted pyrrolo moiety. In general, the spectroscopic features resemble closely that of the pyrroloborane $PBMes_2$ (Scheme 1e) possessing a donor/acceptor strength comparable to DPBN.[20] Furthermore, a strong decrease of the fluorescence rate constants by a factor of 5−10, in comparison with the values found for PBN and PBAEE, can be observed for DPBN (Table 1). The small k_f values indicate a forbidden character of the emission in polar solvents for all three compounds. The strong decrease of k_f for DPBN may be connected with the sterical hindrance by the ortho methyl groups leading to a twisted conformation already in the electronic ground state. In contrast to PBN and PBAEE, the fluorescence intensity of which is quite insensitive to the solvent polarity, a strong fluorescence quenching in highly polar solvents such as acetonitrile and ethanol can be observed for DPBN (Table 1c).

The excited-state dipole moments of PBN and DPBN were determined from the solvatochromic slopes by applying the Lippert−Mataga equation (eq 4).[21] The Onsager radii 4.1 Å for PBN and 4.3 Å for DPBN were estimated by the mass−density formula (eq 5)[22] by taking an average density $\rho = 0.95$ g/cm^3.

$$\Delta\tilde{\nu} = \tilde{\nu}_{abs} - \tilde{\nu}_f = \frac{2\Delta f}{hca^3}(\mu_{S_1} - \mu_{S_0})^2 + \text{const} \qquad (4)$$

$$\text{with} \quad \Delta f = \frac{(\epsilon - 1)}{(2\epsilon + 1)} - \frac{(n^2 - 1)}{(2n^2 + 1)}$$

$$a = \sqrt[3]{3M/4\pi N_A \rho} \qquad (5)$$

The resulting dipole moment differences $\Delta\mu = \mu_{S_1} - \mu_{S_0}$ were determined as 19.2 D for PBN and 18.8 D for DPBN. A similar value results for PBAEE in view of the nearly identical solvent shifts of the emission spectra (Table 1). With an estimation of the ground-state dipole moment taking similar values for all three compounds (3.2 D[23]) we can conclude, that the excited-state dipole moments of all three compounds are close to 22 D.

3.2. Spectroscopic Measurements at Low Temperature. The fluorescence measurements at lower temperatures were done in the nonpolar solvent mixture methylcyclohexane:isopropane (MCH/IPE) and in ethanol, i.e., in solvents forming glasses with reduced light-scattering properties at temperatures below the melting point. The fluorescence spectra and corresponding fluorescence decays of the three compounds turn out to be rather uncomplicated at temperatures down to 173 K. There is only one fluorescence band observable, the fluorescence decay of which is monoexponential (Tables 3, 5).

Despite these simple features, a hint for the existence of a more complex photochemistry is given by the development of the vibrational structure of the PBAEE spectra in MCH/IPE, which shows an unusual behavior upon cooling. Normally, an increase in the intensity of the 0−0 transition and increased structuring occurs when the temperature is decreased. The

TABLE 3: Temperature Dependence of the Photophysical Data of PBN and PBAEE in the Solvent Mixture Methylcyclohexane:Isopentane (1:4)

	PBN				PBAEE			
T/K	λ_{max}^{em}/nm	φ_f	τ_f[a]/ns	k_f[b]/10^7 s^{-1}	λ_{max}^{em}/nm	φ_f	τ_f[a]/ns	k_f[b]/10^7 s^{-1}
298	347	0.027	2.9	0.94	332	0.033	1.4	2.34
273	348	0.030	3.4	0.88	334	0.039	2.4	1.34
253	348	0.035	3.9	0.89	336	0.057	3.4	1.68
233	349	0.039			338	0.065		
213	350	0.046	4.7	0.97	340	0.067	4.3	1.56
193	350	0.049			341	0.071		
173	352	0.050	6.1	0.81	342	0.075	5.5	1.36
77	357		10.8		380		10.2	

[a] For temperatures 77 K < T < 173 K, a multiexponential fit was needed (up to 4 exp). For all other temperatures, a monoexponential fit was sufficient. [b] Calculated from φ_f/τ_f.

TABLE 4: Temperature Dependence of the Photophysical Data of PBN and PBAEE in Ethanol K

		289 K	273 K	253 K	233 K	213 K	193 K	173 K	77 K
PBN	λ_{max}^{em}/nm	478	479	481	484	482	480	477	371
	$\varphi_f \times 10^{-2}$	2.2	2.1	2.0	2.0	2.1	2.3	2.9	
PBAEE	λ_{max}^{em}/nm	500	498	498	496	489	482	475	375
	$\varphi_f \times 10^{-2}$	0.2	0.2	0.2	0.3	0.5	0.7	1.3	

TABLE 5: Temperature Dependence of the Photophysical Data of DPBN in the Solvent Mixture Methylcyclohexane:Isopentane (1:4) and in Ethanol

		298 K	273 K	243 K	211 K	173 K	77 K
MCH/	λ_{max}^{em}/nm	420	418	418	420	420	451
IPE	$\varphi_f \times 10^{-2}$	0.72	0.82	0.88	0.81	1.05	
	τ_f[a]/ns	3.8	3.4	3.5	3.9	4.8	15.4
	k_f[b]/10^7 s^{-1}	0.19	0.24	0.25	0.21	0.22	
EtOH	λ_{max}^{em}/nm	584[c]			580	546	468

[a] For temperatures 77 K < T < 173 K, a multiexponential fit was needed (up to 4 exp). For all other temperatures a monoexponential fit was sufficient. [b] Calculated from to φ_f/τ_f. [c] Fluorescence only observable using a highly concentrated sample solution.

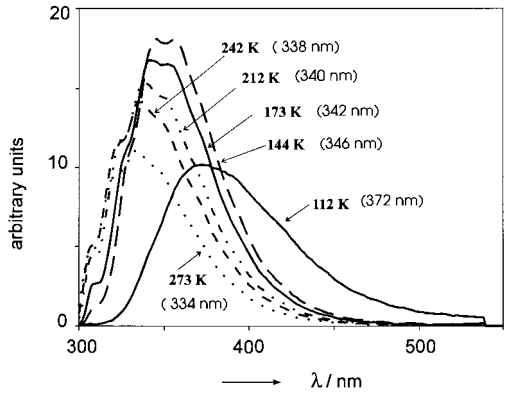

Figure 3. Low-temperature effects on the fluorescence spectra of PBAEE in the nonpolar solvent mixture methylcyclohexane:isopropane (1:4) (wavelength of fluorescence maxima as indicated).

temperature-dependent fluorescence spectra of PBAEE, however, show the opposite effect (Figure 3).

With lowering the temperature, a reduced intensity of the short wavelength shoulder can be observed.

This fact, connected with the observation of a thermochromic red shift of the emission maximum, can serve as a hint for the existence of more than one emitting species with overlapping fluorescence spectra. The population of these excited state species should be thermally equilibrated, because of the observed monoexponential and wavelength-independent decay kinetics. Upon further temperature lowering toward the glass transition point, i.e., at temperatures in the range of 153 to 77 K, the fluorescence decays become multiexponential, reflecting the more complex photophysical behavior of the pyrrolobenzonitrile compounds in rigid environments. This arises because the equilibration of conformations and solute−solvent sites within the excited state is not complete within its lifetime. For these low-temperature conditions, excitation wavelength effects were also found in accordance with corresponding observations on similar compounds in rigid media.[24]

In alcohol, even clearly separated dual fluorescence can be observed (Figure 4a,b), but only in rigid environment conditions below the melting point of ethanol (158.5 K).

At temperatures above 173 K there is only one emission band observable, which exhibits a blue shift upon cooling (Figure 4a). At 153 K a second short wavelength fluorescence with a maximum located at 322 nm is visible, and the long wavelength band shows a further strong blue shift which indicates that solvent relaxation processes are responsible for a large part of the fluorescence red shift observed before. The relative intensity of the short wavelength band grows rapidly with cooling, keeping the excitation wavelength fixed at 280 nm. As demonstrated in Figure 4b, only slight variations of the excitation wavelength give rise to a drastic change of the spectral features, indicating the existence of two close lying excited states, which can be reached in absorption and which do not equilibrate on the time scale of fluorescence emission. Another possibility is the inhomogeneous nature of the absorbing molecular ensemble due to the manifold of different frozen solvent configurations. This effect is well-known as red-edge effect.[24] The broad fluorescence found at longer wavelengths is strongly different from a triplet → singlet transition (phosphorescence) as shown by comparison with the 77 K spectra (Figure 4c).

At 77 K, the phosphorescence with a band maximum at 411 nm exhibits a highly structured spectrum. The fluorescence at 77 K, however, is given by a single, broad and red-shifted emission at 371 nm. The observed fluorescence behavior can be explained by the following model: At 77 K the first excited state can be characterized as a CT state, whereas the second excited state—closely lying in energy but thermally not yet populated significantly—is attributed to a nonpolar LE state (Scheme 2a,b).

Upon warming of the system, there are two competing processes: (i) thermal population of S_2 when k_BT comes close to the S_2-S_1 energy gap ΔE (Scheme 2) and (ii) dipolar solvent relaxation which widens this energy gap because S_1 (CT) is

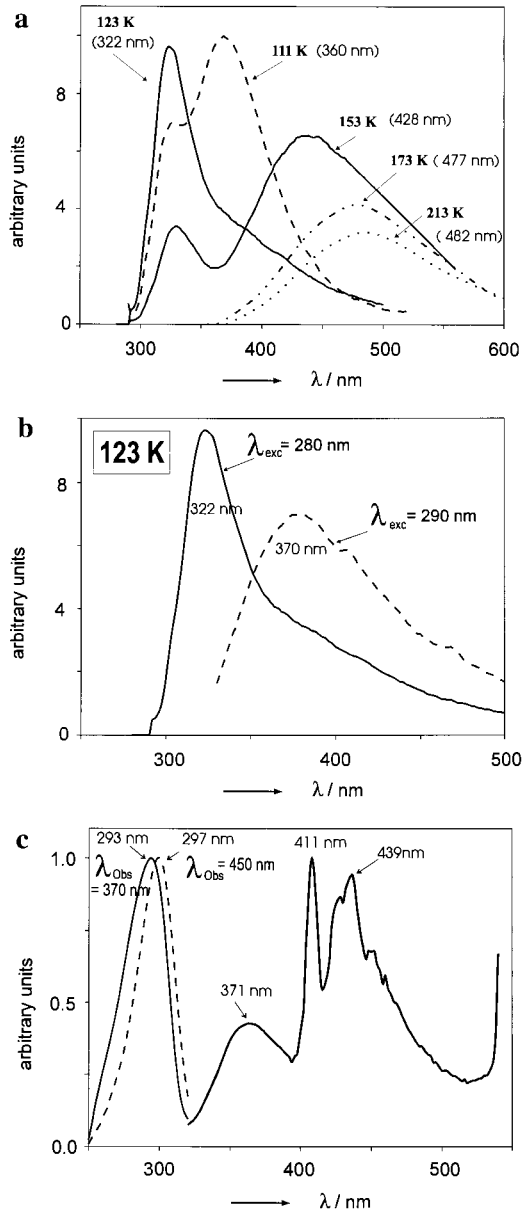

Figure 4. Low-temperature effects on the fluorescence spectra of PBN in ethanol (wavelength of fluorescence maxima as indicated): (a) temperature dependence of the fluorescence spectra with excitation wavelength at 280 nm, (b) variation of the excitation wavelength for PBN in ethanol at 123 K, and (c) excitation and emission spectra measured at 77 K with excitation at 280 nm and observation wavelength as indicated.

more stabilized than S_2. The latter process disfavors thermal population of S_2. Both processes can be observed in the spectra in Figure 4a,c: At 111 K, a distinct band at 320 nm appears which develops into the main band at 123 K, consistent with a thermal population of S_2 (LE). In contrast to the energetically close neighborhood (k_BT) of S_1 and S_2, the fluorescence maxima of both emission bands differ strongly ($\Delta E(\lambda_{max}) \gg k_BT$), indicating that S_1 and S_2 correspond to excited-state species which should possess different molecular conformations (Scheme 2b).

At temperatures approaching the melting point of the solvent, the increased matrix mobility allows some dipolar relaxation processes to occur, which lead to a stabilization of the CT state. This is seen in the redshifted CT band at 153 K in Figure 4a. Under these circumstances, an enlargement of the S_1/S_2 energy gap follows (process (ii)), connected with a diminished probability of thermal population of S_2, and therefore reduction of the intensity of the LE band. At temperatures $T \geq 173$ K, the S_2 state cannot be thermally populated any more, and consequently, only one emission band is observable, which exhibits a large Stokes shift.

SCHEME 2: Different Models for Thermally Populated Excited States ($\Delta E \approx k_BT$): (a) without Structural Relaxation and (b) with Conformational Relaxation Leading to Energy Changes of the Corresponding Franck−Condon Ground States

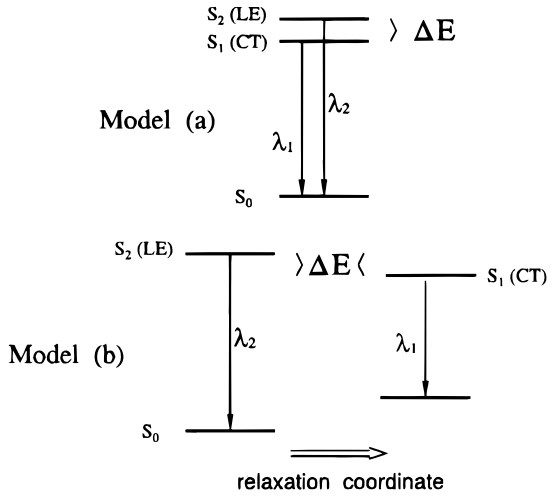

4. Discussion

4.1. Absorption. The compounds investigated can be regarded as substituted benzenes, and the excited states can be classified according to Platt's nomenclature.[25] Donor−acceptor substituted benzenes possess two close lying π,π^* excited states: the long-axis polarized ^1L_a-type state constituting the main long wavelength absorption band and a perpendicularly polarized ^1L_b-type state with much weaker absorption intensity which can cause some structured features in the long wavelength tail of the absorption spectra or which may be completely hidden underneath the much stronger ^1L_a-type band. Depending on the substituents, the role of ^1L_b and ^1L_a as S_1 and S_2 state can interchange.[26] For PBN and PBAEE, the main absorption band can be assigned to the ^1L_a-type excited state. This state is destabilized by twisting as can be concluded from the blue-shifted band in DPBN. This parallels the behavior of twisted biphenyl.[27,28] On the other hand, the ^1L_b-type excited state should also exhibit a weak blue shift upon twisting,[27,29] such that the clearly red-shifted weak shoulder around 350 nm in the absorption spectrum of DPBN cannot be assigned to ^1L_b. We tentatively assign it to a state with high CT character. Due to the symmetry properties of the HOMO of pyrrol and 2,5-dimethylpyrrol with a node through the nitrogen atom,[12] orbital mixing with the HOMO of benzonitrile is not possible, thus the HOMO of PBN and DPBN remain rather localized on the pyrrolo group, independent of the twist angle.[12,13] Excitation from this orbital to the benzonitrile LUMO leads to a state with very large CT character for every twist angle, possibly visible for DPBN in absorption as weak long wavelength shoulder.

4.2. Dual Fluorescence in Nonpolar Solvents. The fluorescence spectra of PBN and PBAEE in the nonpolar solvent *n*-hexane clearly differ from the spectral features in solvents of higher polarity. Apart from the smaller Stokes shift, there is a structuring observable, significant for PBAEE and somewhat weaker for PBN, which indicates that the emission originates,

at least partially, from a nonpolar locally excited state. Additionally, the fluorescence rate constant k_f is significantly larger in nonpolar as compared to polar solvents corresponding to a more allowed character of the emission. The changes of the vibronic structure upon cooling are an indication for the presence of dual emission, i.e., a superposition of the emission from a more allowed LE and a more forbidden CT state. Given the stronger vibronic structure in the hexane spectrum of PBAEE as compared to PBN (Figure 1a,b) and the larger fluorescence rate constant in this solvent as compared to similar values in the other solvents (Table 1), the spectral weight of the LE emission is concluded to be larger for PBAEE than for PBN. The fact that the LE contribution increases with increasing temperature indicates that the reaction free enthalpy ΔG(LE→CT) is negative, i.e., the CT state is more stable than LE even in nonpolar solvents.

4.3. Charge-Transfer Fluorescence in Fluid Polar Solvents. The fluorescence maxima of PBN and PBAEE in more strongly polar solvents as well as those of DPBN in all solvents show a significant red shift with respect to the absorption maxima, leading to Stokes shifts of more than 10 000 cm^{-1}. The strong dependence of the bathochromic shift of the fluorescence band on the solvent polarity scale Δf is rather similar for all compounds, indicating the presence of the same type of emitting highly polar CT state. Although DPBN exhibits a much stronger Stokes shift than PBN, the solvatochromic slope and hence the excited-state dipole moment are similar. The larger Stokes shift can therefore be correlated with the stronger stabilization of the CT state caused by the enhanced donor capability of the dimethyl−pyrrolo moiety as well as with a different emission geometry (see below). The fluorescence rate constants (Table 1; mean value for the radiative lifetime in medium polar solvents: ca. 130 ns in PBN, ca. 120 ns in PBAEE, and ca. 710 ns in DPBN) of the pretwisted derivative DPBN possess significantly smaller values than those measured for PBN and PBAEE although in both cases a pure CT state is emitting. We can therefore conclude that these emitting states probably differ in the mean value of the twist angle in the excited state, with the geometry of the CT state of DPBN being presumably more twisted. This finding is different to what is observed for the prototype TICT molecule DMABN. In this case, the fluorescence rate constants of the CT state are similar for the derivatives with nontwisted and with twisted ground-state geometry,[1,7] and this is evidence that the emitting geometrical structures of the CT state are similar, in accordance with the expectation from the TICT model that the final relaxed CT geometry is perpendicular. In the case of PBN, however, the CT state does not need to relax toward 90° to reach a conformation with full orbital decoupling and maximum CT dipole moment. The relaxed CT conformation may therefore be close to planar and that of DPBN close to perpendicular.

4.4. Dual Fluorescence in Low-Temperature Solvent Glasses. Although there is only one emission band observable in polar solvents at room temperature, a dual emission can be detected upon cooling: below the melting point of the solvent, a second short wavelength fluorescence band occurs. This effect was found for all compounds in ethanol. The relative intensity of both emission bands depends strongly on the temperature and also on the excitation wavelength. At 77 K, however, there is only one fluorescence band observable in the longer wavelength region when exciting at 280 nm (Figure 4c).

The short wavelength emission at about 320 nm is assigned to the energetically close lying S_2 state, which can be thermally populated. The excitation wavelength effects on the dual fluorescence (Figure 4b) and the differing excitation spectra (Figure 4c), however, point to ground-state photoselection combined with incomplete thermal relaxation within the excited-state lifetime. Similar excitation wavelength effects can be observed for DMABN derivatives in polymer glasses or in low-temperature liquid solutions.[24,30] Due to the fact that the maxima of the dual emission at 320 and 370 nm differ by more than kT, the existence of a geometrical relaxation process should be responsible for the energetically distinct position of the fluorescence maxima. Therefore, the emission bands should be assigned to excited-state species possessing different conformations and different ground-state energies (Scheme 2b).

For temperatures above the melting point of the solvent, a relaxation of the solvent molecules takes place connected with the stabilization of the highly polar CT state. This solvent-induced stabilization process causes a larger fluorescence red shift for the CT band as well as the fact that the thermal population of the higher-lying LE state, which is less stabilized than CT, is no longer possible.

This model gains further support by the temperature-dependent changes of the vibrational structure of the PBAEE spectra in nonpolar media. The reduced intensity of the vibronic 0−0 transition as well as the red shift of the complete spectrum can be explained by the existence of two exited-state species whose spectral superposition leads to the temperature effect reported above. Both species remain in thermal equilibrium, which is rapidly reached for $T > 173$ K as is shown experimentally by the monoexponential fluorescence decay in this temperature range. For DPBN, the CT state is energetically more favored, due to the stronger donor capability of the ortho methyl substituted pyrrolobenzonitrile compound. As a consequence, the LE state is no longer thermally populated in nonpolar solvents and the vibronic features in hexane are absent.

Acknowledgment. Support by the Deutsche Forschungsgemeinschaft (Sfb 337) and by the Bundesministerium für Forschung und Technologie (Projects 05 414 FAB1 and 05 5KT FAB9) is gratefully acknowledged.

References and Notes

(1) Grabowski, Z. R.; Rotkiewicz, K.; Siemiarczuk, A.; Cowley, D. J.; Baumann, W. *Nouv. J. Chim.* **1979**, *3*, 443.

(2) Lippert, E.; Rettig, W.; Bonacic-Koutecký, V.; Heisel, F.; Miehé, J. A. *Adv. Chem. Phys.* **1987**, *68*, 1.

(3) Rettig, W. *Modern Models of Bonding and Delocalisation*; Liebman, J. Greenberg, A., Eds.; VCH: New York, 1988; p 229.

(4) Rettig, W. Electron Transfer I. In *Topics in Current Chemistry*; Mattay, J., Ed.; Springer-Verlag, Berlin, 1994; Vol. 169, p 253.

(5) Van der Auweraer, M.; Grabowski, Z. R.; Rettig, W. *J. Phys. Chem.* **1991**, *95*, 2083.

(6) Lippert, E.; Lüder, W.; Boos, H. *Adv. Mol. Spectrosc. Proc. Int. Meet. 4th 1959*, **1962**, *443*.

(7) Rettig, W. *Angew. Chem., Int. Ed. Engl.* **1986**, *25*, 971.

(8) Britelli, D. R.; Eaton, D. F. *J. Phys. Org. Chem.* **1989**, *2*, 89.

(9) Cornelissen-Gude, C.; Rettig, W.; Bonacic-Koutecký, V. Manuscript in preparation.

(10) Schulz, A.; Kaim, W. *Chem. Ber.* **1989**, *122*, 1863. Lequan, M.; Lequan, R. M.; Ching, K. C. *J. Mater. Chem.* **1991**, *1*, 997.

(11) Rettig, W.; Marschner, F. *Nouv. J. Chim.* **1983**, *7*, 425.

(12) Rettig, W.; Marschner, F *New J. Chem.* **1990**, *14*, 819.

(13) Rettig, W. *J. Mol. Struct.* **1982**, *84*, 303.

(14) Frey, H.-P.; Zieloff, K. *Qualitative and quantitative Dünnschichtchromato*graphie; VCH: Weinheim, 1993. Bauer, K.; Gros, Leo; Sauer, W. *Dünnschicht Chromatographie -Einführung*; Merck, Fa., Hüthig, Dr. A., Eds.;Verlag: Weinheim, 1989.

(15) Heinze, J.; Kopf, U. *Anal. Chem.* **1984**, *56*, 1931.

(16) Meech, S. R.; Phillips, D. *J. Photochem.* **1983**, *23*, 193. Velapoldi, R. A.; Epstein, M. S. *ACS Symp. Ser.* **1989**, *383*, 98.

(17) O'Connor, D. V.; Phillips, D. *Time Correlated Single Photon Counting*; Academic Press: London, 1984.
(18) Vogel, M.; Rettig, W. *Ber. Bunsen-Ges. Phys. Chem.* **1987**, *91*, 1241.
(19) Braude, E. A.; Sondheimer, J. *J. Chem. Soc*. **1955**, 3754. Wepster, B. M. *Recueil Trav. Chim. Pays-Bas* **1957**, *76*, 335 and 357.
(20) Cornelissen, C.; Rettig, W. *J. Fluorescence* **1994**, *4*, 71.
(21) Lippert, E. *Z. Naturforschung* **1955**, *10a*, 541. Mataga, N.; Kaifu, Y.; Kazumi, M. *Bull. Chem. Soc. Jpn*. **1955**, *28*, 690; **1956**, *29*, 465.
(22) Rösch, N.; Zerner, M. C. *J. Phys. Chem*. **1994**, *98*, 5817.
(23) Lumbroso, H.; Bertin, D. M.; Marschner, F. *J. Mol. Struct.* **1988**, *178*, 187.
(24) Al-Hassan, K. A.; Rettig, W. *Chem. Phys. Lett.* **1986**, *126*, 273. Al-Hassan, K. A.; Azumi, T.; Rettig, W. *Chem. Phys. Lett*. **1993**, *206*, 25.
(25) Klevens, H. B.; Platt, J. P. *J. Am. Chem. Soc.* **1949**, *71*, 1714.
(26) Rettig, W.; Wermuth, G.; Lippert, E. *Ber. Bunsen-Ges. Phys. Chem*. **1979**, *83*, 692. Wermuth, G. *Z. Naturforsch*. **1983**, *38a*, 368. Wermuth, G.; Rettig, W. *J. Phys. Chem*. **1984**, *88*, 2729.
(27) Suzuki, H. *Electronic Absorption Spectra and Geometry of organic Molecules*; Academic Press: New York, 1964.
(28) Maus, M.; Rettig, W. *Chem. Phys.* **1997**, *218*, 151.
(29) Swiatkowski, G.; Menzel, R.; Rapp, W. *J. Lumin*. **1987**, *37*, 183.
(30) Braun, D.; Rettig, W. *Chem. Phys. Lett*. **1997**, *268*, 110.